

Ultraviolet-ozone irradiation of HPMC thin films: Structural and thermal properties

Nabawia A. Abdel-Zaher¹, Manal T.H. Moselhey² and Osiris W. Guirguis^{*3}

¹Textile Metrology Lab, National Institute for Standards, Giza, Egypt

²Al-Safwa High Institute of Engineering, Cairo, Egypt

³Department of Biophysics, Faculty of Science, Cairo University, Giza, Egypt

(Received December 7, 2016, Revised February 24, 2017, Accepted March 1, 2017)

Abstract. The aim of the work was to evaluate the effect of ultraviolet-ozone (UV-O₃) irradiation with different times on the structure and thermal properties of hydroxypropyl methylcellulose (HPMC) in the form of a thin film to be used as bioequivalent materials according to their important broad practical and medical applications. HPMC thin films were exposed to UV-O₃ radiation in air at a wavelength of 184.9 nm. The beneficial effects of this treatment on the crystallinity and amorphousity regions were followed by X-ray diffraction technique and FTIR spectroscopy. Differential scanning calorimetry, thermogravimetric and differential thermal analyses were used in order to study the thermal properties of HPMC samples following the process of photodegradation. The obtained results indicated that the rate of degradation process was increased with increasing the exposure time. Variations in shape and area of the thermal peaks were observed which may be attributed to the different degrees of crystallinity after exposing the treated HPMC samples. This meant a change in the amorphousity of the treated samples, the oxidation of its chemical linkages on its surface and its bulk, and the formation of free radical species as well as bond formation.

Keywords: HPMC; photodegradation; X-ray diffraction; FTIR spectroscopy; thermal properties

1. Introduction

Hydroxypropyl methylcellulose (HPMC) belongs to group of cellulose ethers, non-toxic and has hydrophilic nature (Hofenk-de Graaff 1981). HPMC has been used for a year by paper of conservators as glue, sizing and adhesives (Paradossi *et al.* 2003). According to the versatile properties of HPMC biopolymer, many applications in the food, cosmetic, and pharmaceutical industries were found. HPMC was used in the hydrogel technology and has emerged as a good substitute as a coating/film for drug delivery due to its hydrophilic nature (Siepmann and Peppas 2008, Ferrero *et al.* 2010, Gendre *et al.* 2011, Ku *et al.* 2011, Maderuelo *et al.* 2011, Yinghui Wei *et al.* 2012).

Due to the ability of HPMC to form a colloidal solution, it was also used as a drug carrier, and as an emulsifier for pharmaceutical creams as well as cosmetic lotions. It was used in hair care,

*Corresponding author, Ph.D., E-mail: osiris_wgr@yahoo.com

onto stainless steel Petri dishes (10 cm in diameter) and kept at room temperature ($\approx 25^\circ\text{C}$) for 7 days until the water completely evaporated. Finally, thin transparent HPMC films of about 0.01 cm in thickness were formed and then kept in desiccators containing fused calcium chloride to avoid moisture.

The prepared HPMC thin films are exposed to UV-O₃ with different exposure times (1, 2, 3 and 4 h). High intensity, low-pressure mercury lamp without outer envelope -LRF 02971, 200 watt, 220 volt (Poland) placed in a cubic box with side length 60 cm was used as the UV-O₃ source at National Institute for Standards, Giza, Egypt. Atomic oxygen is generated both when molecular oxygen is subjected to the 184.9 nm radiation and when ozone was irradiated at 253.7 nm. The 253.7 nm radiation was absorbed by most hydrocarbons and also by ozone (Michael *et al.* 2004, Smith 2011, Abdel-Zaher *et al.* 2016). The samples of dimensions 1×4 cm were placed around the source at a distance 20 cm.

2.2 Characterizations of the prepared HPMC films

2.2.1 X-ray diffraction (XRD)

The XRD of HPMC films was measured by using a Phillips PW1840 X-Ray Diffractometer (USA) with an anode tube of CuK_α radiation ($\lambda=1.54056 \text{ \AA}$), operated at 40 kV and 25 mA. The patterns were recorded in the range of 2θ from 5 to 90° at a speed rate of 2 degrees/minute. The crystallinity index (CrI) (i.e., the time-save empirical measure of relative crystallinity) of the sample was calculated using the relation (Segal *et al.* 1959)

$$\text{CrI} = [(I_f - I_s)/I_f] \times 100 \quad (1)$$

Where I_f is the peak intensity of the fundamental band and I_s is the peak intensity of the secondary band.

2.2.2 Fourier transform infrared (FTIR) spectroscopy

The absorption spectra of the prepared HPMC films over the range 4000-500 cm^{-1} were performed by using Fourier transform infrared (FTIR) Spectrophotometer, model Bruker Vector 22 (Germany) with accuracy better than $\pm 1\%$.

2.2.3 Thermal analyses

The thermal properties of the prepared HPMC films were analyzed by using Differential Scanning Calorimetry (DSC) model Shimadzu DSC-50 (Kyoto, Japan) and Thermogravimetric Analyzer model Shimadzu TGA-50H (Kyoto, Japan). The DSC, TGA and DTA analyses cover the range from 25 to 650°C were performed under nitrogen atmosphere of rate of flow 20 mL/minute and at rate of heating of $10^\circ\text{C}/\text{minute}$. The average weight of the sample was about 6 mg. The standard uncertainty of the sample weight measurement was $\pm 1\%$ and the instrument was calibrated using calcium oxalate.

3. Results and discussion

3.1 X-ray diffraction analysis

The XRD patterns of unexposed and UV-O₃ exposed HPMC films were shown in Fig. 1. The pattern of unexposed HPMC sample showed amorphous features characterized by two different

Ultraviolet-ozone irradiation of HPMC thin films: Structural and thermal properties

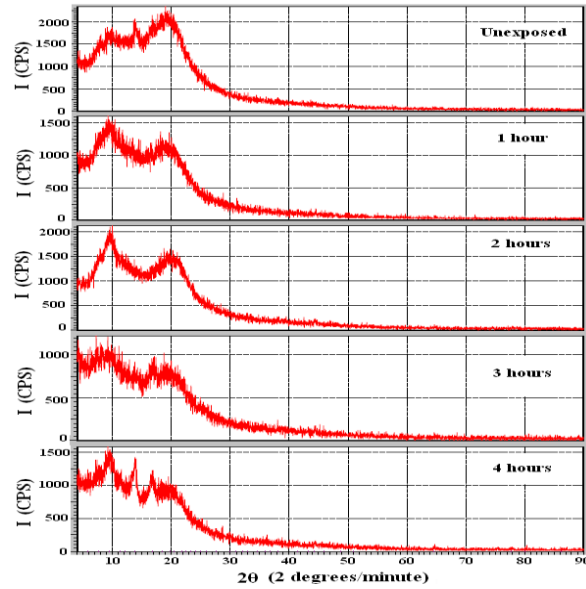


Fig. 1 XRD patterns of unexposed and exposed HPMC films

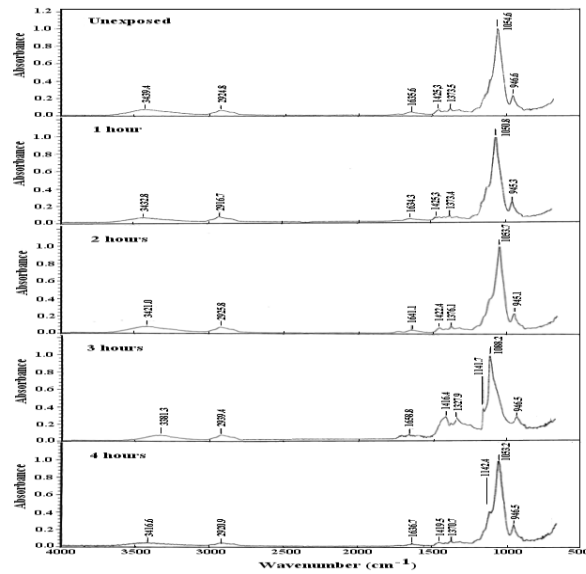


Fig. 2 Variations in FTIR spectra of unexposed and exposed HPMC films

the induced effect of exposure time on the structure of HPMC (El-Zaher and Osiris 2005).

3.2 FTIR spectral analyses

The FTIR absorbance spectra of HPMC samples as functions of wavenumber in the range $4000\text{-}500\text{ cm}^{-1}$ were shown in Fig. 2. The chemical assignments were considered and were illustrated in Table 2.

Table 3 Values of transition temperatures and associated heat of fusion for unexposed and exposed HPMC films

HPMC films	At melting transition region			
	First step		Second step	
	T_m (°C)	ΔH_m (J/g)	T_m (°C)	ΔH_m (J/g)
Unexposed	327.8	78.76	528.8	139.17
1	379.1	49.01	524.1	128.66
2	419.7	50.22	536.1	118.03
3	368.4	36.21	530.2	76.97
4	399.4	34.04	530.2	76.97
	415.0	-9.05	Not detected	

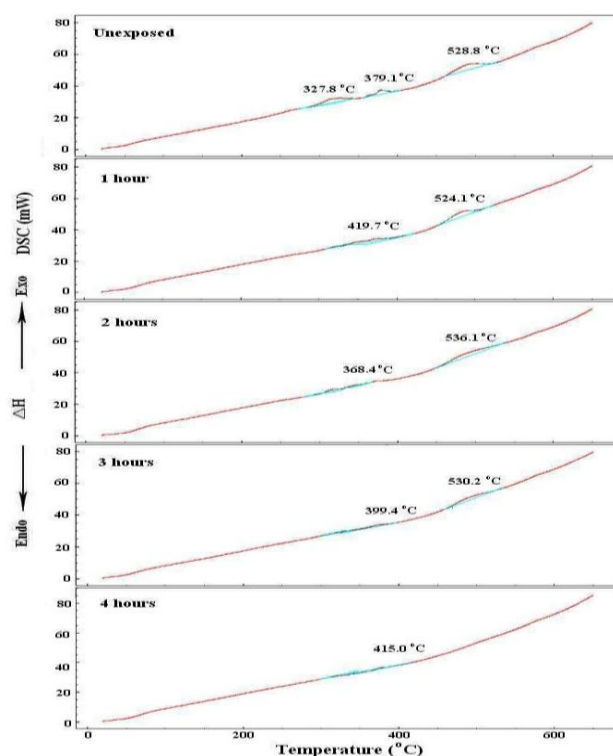


Fig. 3 DSC curves for unexposed and exposed HPMC films

play a dominant role in deciding the rigidity of the structure and also associated with the change in degradation and/or cross-linkage and coordination of the polymer network (Bernard *et al.* 2003, Osiris and Manal 2011).

3.3 Thermal analyses

3.3.1 Differential scanning calorimetry (DSC)

The glass transition temperature, crystallization temperature, heat of crystallization, melting

Table 5 The total % weight loss and the residue % of unexposed and exposed HPMC films

HPMC films UV-O ₃ exposure times (h)	Total % weight loss	Residue %
Unexposed	80.037	19.963
1	90.548	9.452
2	87.103	12.897
3	87.404	12.596
4	87.718	12.282

found in the samples with different exposure times.

Table 3 depicts the melting transition temperatures and the heat of fusion (ΔH_m) of each transition obtained through the analysis of DSC curves for both unexposed HPMC sample as well as of samples after different times of UV-O₃ exposure. It was clear from the table that, two melting transition temperatures were detected except the 4 h exposed sample which showed one single value. In addition, while the time of irradiation increases, the values of melting temperatures of exposure HPMC samples increase and the values of heat of fusion decrease. As reported in literatures that, melting of polymers was depended on the degree of crystallinity, ordering of macromolecules and molecular weight of the polymer (Bras *et al.* 2007). In the DSC curves of HPMC samples, two melting transition temperatures were detected. This observation can be explained by coexistence of more than one degradation process of melting which was typical of bimodal polymers (Song *et al.* 2013). Moreover, a change in the crystalline structure could be due to polymer interactions in the amorphous phase, and then disorder in the crystals was created reducing the enthalpy of the phase change (Hammel *et al.* 1975).

3.3.2 Thermogravimetric (TGA) and differential thermal (DTA) analyses

Thermal degradation behaviors of unexposed and exposed HPMC were examined by thermogravimetric analyses (TGA) as shown in Fig. 4. In addition, the difference in thermal decomposition behaviors of the unexposed and exposed HPMC samples can also be seen from the differential thermal analyses (DTA) curves (Fig. 4). It is clear from the figure for both TGA and DTA analyses that, the degradation behaviors of the photodegradation of HPMC samples were almost similar to the behavior of the unexposed one. Two decomposition stages were recorded for both unexposed and exposed HPMC samples which suggested the coexistence of more than one degradation process. In addition, a reduction of HPMC sample decomposition temperatures along with the increase in photodegradation time.

Table 4 depicts the TGA data for unexposed and exposed HPMC films with UV-O₃ for different exposure times. It was noticed from the table for the unexposed and exposed HPMC samples that the first decomposition stage (i.e., at the first order thermodynamic transition region) showed lower values of % weight loss (3.450-5.199). More significant values of % weight loss (76.587-82.519) were detected for the second decomposition stage (i.e., at the melting transition region). Before UV radiation the first decomposition temperature of HPMC sample equaled about 44°C and non-remarkable decreased to about 43°C after 4 h of irradiation. The first decomposition temperature depends on the structure of the polymer chain, its elasticity and the molecular weight of the polymer (Ewa Olewnik-Kruszkowska 2015). The lower values of % weight loss in the first order thermodynamic transition region started at about 40°C confirm the presence of a thermal

References

- Abd El-Kader, F.H., Gaafar, S.A., Mahmoud, K.H., Bannan, S.I. and Abd El-Kader, M.F.H. (2008), “ γ -irradiation effects on the thermal and optical properties of undoped and eosin doped 70/30 (wt/wt%) PVA/glycogen films”, *Curr. Appl. Phys.*, **8**(1), 78-87.
- Bernard, C., Chaussedent, S., Monteil, A., Montagna, M., Zampedri, L. and Ferrari, M. (2003), “Simulation by molecular dynamics of erbium-activated silica-titania glasses”, *J. Sol-Gel Sci. Technol.*, **26**(1), 925-929.
- Bolon, D.A. and Kunz, C.O. (1972), “Ultraviolet depolymerization of photoresist polymers”, *Polym. Eng. Sci.*, **12**(2), 109-111.
- Bras, A.R., Viciosa, M.T., Dionisio, M. and Mano, J.F. (2007), “Water effect in the thermal and molecular dynamics behaviour of poly(l-lactic acid)”, *J. Therm. Anal. Calorimet.*, **88**(2), 425-429.
- Chiu, J. (1966), “Applications of thermogravimetry to the study of high polymers”, *Appl. Polym. Symp.*, **2**, 25-43.
- Cullis, C.F. and Hirschler, M.M. (1981), *Combustion of Organic Polymers*, Clarendon Press, Oxford, U.K.
- Desai, R.L. and Shields, J.A. (1969), “Photochemical degradation of cellulose material”, *Die Makromol. Chem.*, **122**(1), 134-144.
- El-Zaher, N.A. and Osiris, W.G. (2005), “Thermal and structural properties of poly(vinyl alcohol) doped with hydroxypropyl cellulose”, *J. Appl. Polym. Sci.*, **96**(5), 1914-1923.
- Ewa, O.K. (2015), “Effect of UV irradiation on thermal properties of nanocomposites based on polylactide”, *J. Therm. Anal. Calorimet.*, **119**(1), 219-228.
- Ferrero, C., Massuelle, D. and Doelker, E. (2010), “Towards elucidation of the drug release mechanism from compressed hydrophilic matrices made of cellulose ethers: II. Evaluation of a possible swelling-controlled drug release mechanism using dimensionless analysis”, *J. Control. Rel.*, **141**, 223-233.
- Gendre, C., Boiret, M., Genty, M., Chaminade, P. and Pean, J.M. (2011), “Real time predictions of drug release and end point detection of a coating operation by in-line near infrared measurements”, *J. Pharm.*, **421**(2), 237-243.
- Hammel, R., MacKnight, W.J. and Karasz, F.E. (1975), “Structure and properties of the system: Poly(2,6-dimethyl-phenylene oxide) isotactic polystyrene wide-angle x-ray studies”, *J. Appl. Phys.*, **46**(10), 4199-4203.
- Hofenk-de, G.J. (1981), *Central Research Laboratory for Objects of Art and Science*, Gabriel Metsustraat and 1071 EA, Amsterdam, the Netherlands.
- Kim, J.H., Kim, J.Y., Lee, Y.M. and Kim, K.Y. (1992), “Properties and swelling characteristics of cross-linked poly(vinyl alcohol)/chitosan blend membrane”, *J. Appl. Polym. Sci.*, **45**(10), 1711-1717.
- Ku, M.S., Lu, Q., Li, W. and Chen, Y. (2011), “Performance qualification of a new hypromellose capsule: Part II. Disintegration and dissolution comparison between two types of hypromellose capsules”, *J. Pharm.*, **416**(1), 16-24.
- Lim, S.L., Fane, A.G. and Fell, C.J.D. (1990), “Radiation-induced grafting of regenerated cellulose hollow-fiber membranes”, *J. Appl. Polym. Sci.*, **41**(7-8), 1609-1616.
- Maderuelo, C., Zarzuelo, A. and Lanao, J.M. (2011), “Critical factors in the release of drugs from sustained release hydrophilic matrices”, *J. Control. Rel.*, **154**(1), 2-19.
- Madhu Mohan, V., Raja, V., Sharma, A.K. and Narasimha Rao, V.V.R. (2005), “Ionic conductivity and discharge characteristics of solid-state battery based on novel polymer electrolyte (PEO+NaBiF₄)”, *Mater. Chem. Phys.*, **94**(2), 177-181.
- METHOCEL Cellulose Ethers (2002), *Technical Handbook*, Trademark of the Dow Chemical Company, U.S.A.
- Michael, M.N., El-Zaher, N.A. and Ibrahim, S.F. (2004), “Investigation into surface modification of some polymeric fabrics by UV/ozone treatment”, *Polym.-Plast. Technol. Eng.*, **43**(4), 1041-1052.
- Nabawia, A., Abdel-Zaher, M.T.H. and Osiris, W.G. (2016), “Optical studies of hydroxypropyl methylcellulose thin films exposed to UV/ozone”, *J. Sci. Eng. Res.*, **3**, 84-96.

- Neto, C.G.T., Giacometti, J.A., Job, A.E., Ferreira, F.C., Fonseca, J.L.C. and Pereira, M.R. (2005), "Thermal analysis of chitosan based network", *Carbohydr. Polym.*, **62**(2), 97-103.
- Osiris, W.G. and Manal, T.H.M. (2011), "Optical study of poly(vinyl alcohol)/hydroxypropyl methylcellulose blends", *J. Mater. Sci.*, **46**(17), 5775-5789.
- Paradossi, G., Cavalieri, F., Chiessi, E., Spagnoli, C. and Cowman, M.K. (2003), "Poly(vinyl alcohol) as versatile biomaterial for potential biomedical applications", *J. Mater. Sci.: Mater. Medic.*, **14**(8), 687-691.
- Park, C.K., Choi, M.J. and Lee, Y.M. (1995), "Chelate membrane from poly(vinyl alcohol)/poly(*N*-salicylidene allyl amine) blend. I: Synthesis and characterization of Co(II) chelate membrane", *Polym.*, **37**, 1507-1512.
- Qiangzhong, Z., Mouming, Z., Jianrong, L., Bao, Y., Guowan, S., Chun, C. and Yueming, J. (2009), "Effect of hydroxypropyl methylcellulose on the textural and whipping properties of whipped cream", *Food Hydrocol.*, **23**(8), 2168-2173.
- Quoc, T.L., Whelan, C.M., Struyf, H., Vanhaelemeersch, S., Azioune, A., Louette, P., Pireaux, J.J. and Maex, K. (2004), "Polymer dielectric treatment using ultraviolet-ozone: A photoelectron spectroscopy and ellipsometric porosimetry study", *J. Appl. Phys.*, **96**(7), 3807-3810.
- Sakellariou, P., Hassan, A. and Rowe, R.C. (1993), "Phase separation and polymer interactions in aqueous poly(vinyl alcohol)/hydroxypropyl methylcellulose blends", *Polym.*, **34**(6), 1240-1248.
- Schulz, M.B. and Daniels, R. (2000), "Hydroxypropyl methylcellulose (HPMC) as emulsifier for submicron emulsions: Influence of molecular weight and substitution type on the droplet size after high-pressure homogenization", *Eur. J. Pharmac. Biopharmac.*, **49**(3), 231-236.
- Segal, L., Creely, J.J., Martin Jr, A.E. and Conrad, C.M. (1959), "An empirical method for estimating the degree of crystallinity of native cellulose using the x-ray diffractometer", *Text. Res. J.*, **29**(10), 786-794.
- Siepmann, J. and Peppas, N.A. (2001), "Modeling of drug release from delivery systems based on hydroxypropyl methylcellulose (HPMC)", *Adv. Drug Del. Rev.*, **48**, 139-157.
- Smith, A.L. (1979), *Applied Infrared Spectroscopy, Fundamentals Techniques and Analytical Problem-Solving*, Wiley, New York, U.S.A.
- Smith, B.C. (2011), *Fundamentals of Fourier Transform Infrared Spectroscopy*, 2nd Edition, CRC Press, Boca Raton, London, New York, U.S.A.
- Song, P., Chen, G., Wei, Z., Zhang, W. and Liang, J. (2013), "Calorimetric analysis of the multiple melting behavior of melt-crystallized poly(L-lactic acid) with a low optical purity", *J. Therm. Anal. Calorimet.*, **111**(2), 1507-1514.
- Yinghui, W., Xiaoli, Y., Xiaoguang, S., Xuan, P., Qiang, B., Minchen, L., Manman, G. and Fanzhu, L. (2012), "Enhanced oral bioavailability of silybin by a supersaturatable self-emulsifying drug delivery system (S-SEDDS)", *Coll. Surf. A: Physicochem. Eng. Asp.*, **396**, 22-28.
- Yukoh, S., Sumihiro, S. and Makoto, O. (2006), "A novel white film for pharmaceutical coating formed by interaction of calcium lactate pentahydrate with hydroxypropyl methylcellulose", *J. Pharm.*, **317**(2), 120-126.